

Nucleon spectral function in complex nuclei and nuclear matter and inclusive quasielastic electron scattering

C. Ciofi degli Atti,^(1,2) S. Liuti,⁽²⁾ and S. Simula⁽²⁾

⁽¹⁾*Physics Department, University of Perugia, Via A. Pascoli, I-06100 Perugia, Italy*

⁽²⁾*Istituto Nazionale di Fisica Nucleare, Sezione Sanità, Viale Regina Elena 299, I-00161 Rome, Italy*

(Received 9 February 1990)

Inclusive quasielastic electron scattering by few-body systems, complex nuclei, and nuclear matter is analyzed in terms of y scaling using a nucleon spectral function which incorporates the momentum and removal energy distributions generated by two-nucleon correlations. It is demonstrated that binding effects play a relevant role in y scaling and that a qualitative interpretation of the available experimental data would require the simultaneous consideration of ground-state correlations and final-state interaction effects.

Since the work by West,¹ there was an increase of interest in inclusive quasielastic (QE) electron scattering in the kinematics pertaining to y scaling. It has been shown, in particular,² that, using nonrelativistic kinematics and assuming the validity of the plane-wave impulse approximation (PWIA), the nuclear structure function (scaling function) coincides in the limit $q \rightarrow \infty$ (q being the three momentum transfer) with the longitudinal momentum distribution. Such a direct link between these two quantities is, however, destroyed by the use of relativistic kinematics.³ Moreover, it should be reiterated that at finite values of the momentum transfer the nuclear structure function in inclusive QE scattering is never linked, even within the PWIA, to the longitudinal momentum distribution, unless all nucleons in the target are considered to be bound with the same value of the energy. The calculation of inclusive QE cross section both at finite and infinite momentum transfer does require the knowledge of the nucleon spectral function $P(k, E)$, i.e., the momentum (k) and removal energy (E) distributions of nucleons imbedded in the nuclear medium. A thorough analysis of y scaling in terms of a realistic spectral function exists to date only for the three nucleon system. With the recent advent of experimental data on QE cross section for complex nuclei,^{4,5} the necessity of their analysis in terms of the spectral function is a prerequisite for any progress in this field. In Ref. 6 the experimental data for ⁵⁶Fe have been compared with a theoretical calculation based upon the dilute hard-sphere Fermi gas. In this Rapid Communication the experimental data for ⁴He, ¹²C, ⁵⁶Fe, and nuclear matter are instead analyzed in terms of the spectral function proposed in Ref. 7, which incorporates the momentum and removal energy distributions arising from nucleon-nucleon (NN) correlations. Such a spectral function, whose basic ingredients will be briefly illustrated here below, results from an extension of the few-nucleon-correlation (FNC) model of Ref. 8.

When NN correlations are considered, the spectral function can be represented as follows:

$$P(k, E) = P_0(k, E) + P_1(k, E), \quad (1)$$

where P_0 includes the ground and one-hole states of the residual ($A-1$) system and P_1 more complex configurations (mainly one-particle-two-hole states) which arise from two-particle-two-hole states generated in the ground state of the nucleus A by NN correlations. In what follows the following forms will be adopted:⁹

$$P_0(k, E) = 1/(4\pi A) \sum_a A_a n_a(k) \delta(E - |\epsilon_a|) \quad (2)$$

and

$$P_1(k, E) = (2\pi)^{-3} \sum_{f \neq a} \left| \int d\mathbf{r} e^{i\mathbf{k} \cdot \mathbf{r}} G_{f0}(\mathbf{r}) \right|^2 \delta(E - E_f^i), \quad (3)$$

where $E_f^i \equiv E_{A-1}^* + E_{\min}$, $E_{\min} = M + M_{A-1} - M_A$, E_{A-1}^* is the (positive) excitation energy of the residual ($A-1$) system, n_a is the momentum distribution of the shell model single-particle (SP) state a [with SP energy ϵ_a and number of nucleons A_a ($\sum_a A_a = A$)], and finally $G_{f0}(\mathbf{r})$ is the overlap integral between the wave function of the ground state of the nucleus A and the wave function of the state $f \neq a$ of the nucleus ($A-1$). In Eq. (2) the sum over a runs only over hole states and in Eq. (3) the sum over f also includes the integration over continuum states. Within the Hartree-Fock (HF) approximation $P_1(k, E) = 0$, and the HF spectral function, i.e., Eq. (2) with $n_a(k) = n_a^{\text{HF}}(k)$ is recovered. The occupation number of the state i is $c_i \equiv \int n_i(k) k^2 dk < 1$ and $c_i^{\text{HF}} \equiv \int n_i^{\text{HF}}(k) \times k^2 dk = 1$, for hole states, and $c_i > 0$ and $c_i^{\text{HF}} = 0$, for particle states. The spectral function and the momentum distribution $n(k)$ are related by the momentum sum rule¹⁰ which leads, in the specific case of the spectral function (1), to

$$n(k) = 4\pi \int_{E_{\min}}^{\infty} P(k, E) dE = 4\pi \int_{E_{\min}}^{\infty} P_0(k, E) dE + 4\pi \int_{E_{\min}}^{\infty} P_1(k, E) dE = n_0(k) + n_1(k). \quad (4)$$

For an extended system like nuclear matter, the hole part of the spectral function can be cast in the following form:¹¹

$$P_0^{\text{NM}}(k, E) = 3/(4\pi k_F^3) Z(k) \Theta(k_F - k) \delta(E + e(k)), \quad (5)$$

where $Z(k)$ is the hole strength, $e(k)$ the hole-single-particle spectrum, and k_F the Fermi momentum [in absence of NN correlations $e(k) = k^2/2M$, $Z(k) = 1$, and the usual Fermi gas spectral function is recovered]. Calculations in the three-nucleon system¹⁰ and nuclear matter¹¹ show that the behavior of the spectral function at high values of k and E is almost entirely governed by P_1 ; the approach of Ref. 7 aims at providing a realistic model for this quantity starting from the observation that the perturbative expansion for the NN interaction and the nucleon momentum distribution,⁸ as well as the direct calculation of Eq. (3) for different values of the upper limit of integration (see Fig. 3 of Ref. 10), clearly show that at high values of nucleon momentum and removal energies, the spectral function is governed mainly by the process

$$P_1(k, E) = (4\pi)^{-1} n_1(k) N \exp\{-(2\sigma^2)^{-1} [\sqrt{M(E - E_{\text{thr}})} - \sqrt{M(E_1(k) - E_{\text{thr}})}]^2\}, \quad (7)$$

where N is a proper normalization constant [such that $4\pi \int dE P_1(k, E) = n_1(k)$], $E_{\text{thr}} = |E_A| - |E_{A-2}|$ is the two-body breakup threshold and the full width at half maximum $\Gamma(k)$ is given by

$$\Gamma(k) = 4\sigma \sqrt{(2 \ln 2) E_1(k) / M} = \langle E \rangle_1 + E_1(k), \quad (8)$$

where $\langle E \rangle_1 = \int E dE P_1(k, E)$. The above spectral function, whose theoretical validation is discussed elsewhere,⁷ satisfies the momentum [Eq. (4)] and energy¹² sum rules; is free from any adjustable parameters; is expressed through many-body quantities, e.g., $n_1(k)$ and $\langle E \rangle_1$, which have been calculated for few-body systems, complex nuclei, and nuclear matters in terms of realistic NN interactions. For ${}^3\text{He}$ and nuclear matter, Eq. (7) is in excellent agreement with the many-body results of Refs. 10 and 11. The full spectral function (1) for ${}^4\text{He}$, ${}^{12}\text{C}$, ${}^{56}\text{Fe}$, and nuclear matter has been obtained using P_0 in the forms (2) and (5), and P_1 in the form (7); the momentum distributions $n_0(k)$ and $n_1(k)$, and the value of $\langle E \rangle_1$ have been taken from Ref. 11 (nuclear matter), Ref. 13 (${}^4\text{He}$), and Ref. 14 (${}^{12}\text{C}$), which yield on the average $\int n_0(k) k^2 dk = 0.8$ and $\int n_1(k) k^2 dk = 0.2$ for ${}^4\text{He}$ and ${}^{12}\text{C}$, and $\int n_0(k) k^2 dk = 0.75$, $\int n_1(k) k^2 dk = 0.25$ for nuclear matter; for ${}^{56}\text{Fe}$ we have chosen $n_0(k) = 0.8n^{\text{HF}}(k)$ and $n_1(k) = n(k) - n_0(k)$, with $n(k)$ from Ref. 6. The values of hole energies were taken from ($e, e'p$) experiments.¹⁵ In order to illustrate the relevant role played by the removal energy dependence of $P(k, E)$, the saturation properties of the momentum sum rule for ${}^3\text{He}$, ${}^{12}\text{C}$, and nuclear matter are reported in Fig. 1, which clearly shows that the trend previously observed in ${}^3\text{He}$ (Ref. 10) and nuclear matter,¹¹ namely that the high-momentum components are strictly linked with high values of the removal energy, holds in finite nuclei as well; it can also be seen that the predictions of our spectral function very satisfactorily agree with the ones by many-body calculations. The nuclear structure function (scaling function), which appears in the definition of the inclusive

(two-nucleon correlations, according to Ref. 8) in which the momentum $\mathbf{k}_1 \equiv \mathbf{k}$ of a high-momentum nucleon (the *hard* nucleon) is balanced only by the momentum $\mathbf{k}_2 \equiv -\mathbf{k}$ of another nucleon, with the remaining $(A-2)$ nucleons (the *soft* nucleons) acting as spectators with total momentum $\mathbf{k}_{A-2} \equiv 0$. Such a picture leads to a spectral function P_1 in the form of a δ function $\delta(E - E_1(k))$, with $E_1(k)$ determined from the following equation:

$$(M_{A-1}^*{}^2 + k^2)^{1/2} = (M^2 + k^2)^{1/2} + M_{A-2}, \quad (6)$$

where $M_{A-1}^* = M_A - M + E_1(k)$. By allowing the spectator $(A-2)$ system to share momentum with the hard nucleon, the spectral function will acquire a removal energy and momentum dependence for $E \neq E_1(k)$, which, in Ref. 7, has been assumed to be of the following form:

cross section in PWIA, is given by¹⁶

$$F(y, q) = 2\pi \sum_a \int_{k_{\min}(y, q, \epsilon_a)}^{k_{\max}(y, q, \epsilon_a)} n_a(k) k dk + 2\pi \int_{E_{\min}}^{E_{\max}(y, q)} dE \int_{k_{\min}(y, q, E)}^{k_{\max}(y, q, E)} P_1(k, E) k dk, \quad (9)$$

where the limits of integration are fixed by the energy conservation

$$\omega + M_A = [M^2 + (\mathbf{k} + \mathbf{q})^2]^{1/2} + (M_{A-1}^*{}^2 + k^2)^{1/2}, \quad (10)$$

where $\omega(\mathbf{q})$ is the energy (three momentum) transfer. The scaling variable $y = f(q, \omega)$ is $|y| = k_{\min}(q, \omega, E_{\min})$, i.e., the solution of

$$\omega + M_A = [M^2 + (q + y)^2]^{1/2} + (M_{A-1}^*{}^2 + y^2)^{1/2}. \quad (11)$$

In the asymptotic limit $q \rightarrow \infty$, one has

$$F(y) = 2\pi \sum_a \int_{k_{\min}(y, \epsilon_a)}^{\infty} n_a(k) k dk + 2\pi \int_{E_{\min}}^{\infty} dE \int_{k_{\min}(y, E)}^{\infty} P_1(k, E) k dk, \quad (12)$$

with³

$$k_{\min}^{\infty}(y, E) = \left| y + \frac{M_{A-1}^*{}^2 - M_{A-2}^*{}^2}{2\{y + (y^2 + M_{A-1}^*{}^2)^{1/2}\}} \right|. \quad (13)$$

As reiterated in Ref. 16, the asymptotic scaling function scales in y but differs from the longitudinal momentum distribution

$$f(y) = 2\pi \int_{E_{\min}}^{\infty} dE \int_{|y|}^{\infty} P(k, E) k dk = 2\pi \int_{|y|}^{\infty} n(k) k dk, \quad (14)$$

the difference depending upon the role played by nucleon binding in QE scattering. We have compared the theoret-

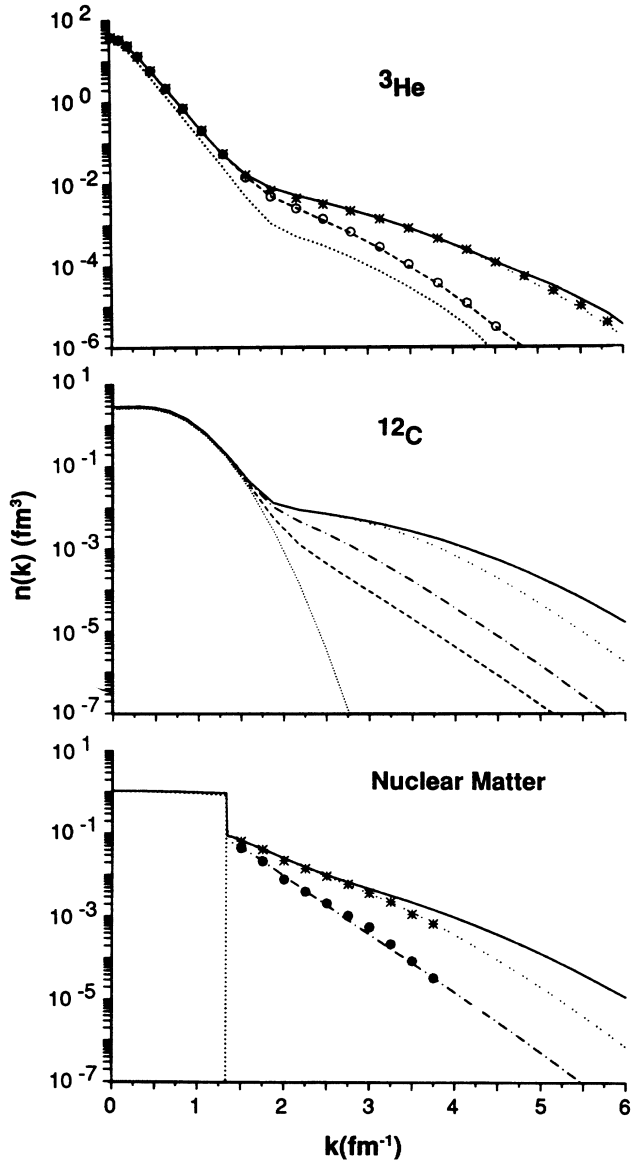


FIG. 1. The saturation of the momentum sum rule (4). The dotted line represents $n_0(k)$ calculated in Ref. 10 (${}^3\text{He}$), Ref. 11 (nuclear matter), and Ref. 14 (${}^{12}\text{C}$), respectively. The dashed, dash-dotted, and double-dotted lines represent Eq. (4) calculated with the spectral function defined by Eqs. (1), (2), (5), and (7), fixing the upper limit of integration equal to $E_{\text{max}} = 50, 100,$ and 300 MeV, respectively; the circles, filled circles, and stars represent the same quantity obtained in Ref. 10 (${}^3\text{He}$) and Ref. 11 (nuclear matter) using many-body spectral functions. The solid line is the total momentum distribution (4). The results presented in this figure for ${}^3\text{He}$ and nuclear matter are taken from Ref. 7.

ical scaling function (9) with the experimental one

$$F^{\text{exp}}(y, q) = \frac{\sigma_2^{\text{exp}}(y, q)}{[Z\sigma_{ep}(y, q) + N\sigma_{en}(y, q)]} K(y, q) \quad (15)$$

obtained in Ref. 17 using for σ_2^{exp} the experimental data from Refs. 4 and 5, for σ_{eN} the off-shell relativistic electron-nucleon cross section of Ref. 18, and for $K(y, q)$

the phase space factor of Ref. 16, viz., $K(y, q) = q/[M^2 + (q + y)^2]^{1/2}$. The comparison between Eqs. (9) and (15) is a significant one, for, if the PWIA is the dominant underlying mechanism of QE scattering, $F^{\text{exp}}(y, q)$ should coincide with $F(y, q)$. It should be pointed out that in Ref. 6, a different prescription has been used to obtain the scaling function and the scaling variable, namely the energy conservation has been approximated by the one in which k^2 in the second term of the right-hand side of Eq. (10) has been disregarded with respect to M_A^{*2} ; such a procedure is strictly valid for nuclear matter only, in which case the equations for E_{max} , k_{min} , k_{max} , and y used in Ref. 6 coincide with ours; for finite nuclei the scaling functions obtained with the exact energy conservation (10) appreciably differ, particularly at large values of $|y|$, from the ones of Ref. 6. The comparison between the theoretical and experimental scaling functions, which is presented in Fig. 2, clearly shows the same trend previously observed in ${}^3\text{He}$, namely, whereas at $y=0$ [i.e., $\omega = (q^2 + M^2)^{1/2} - M + E_{\text{min}} \approx \omega_{\text{peak}}$], nucleon binding plays a minor role and the data qualitatively agree with theoretical calculations, at high negative values of y the following A -independent features can be observed as in the case of ${}^3\text{He}$:¹⁶ (i) the scaling function is almost entirely given by the correlation contribution due to P_1 , so that the HF result is lower than the experimental data by several orders of magnitude; (ii) the longitudinal momentum distribution strongly overestimates the experimental data and appreciably differs from the asymptotic scaling function; (iii) even when correlations are considered, an appreciable discrepancy between experimental data and theoretical calculations occurs, which decreases with momentum transfer. Such a discrepancy is a clear manifestation of the effects from final-state interaction (FSI); as a matter of fact, according to PWIA the theoretical scaling function should increase with momentum transfer, whereas the experimental data decrease with q ; (iv) for fixed values of y , the q dependence of the experimental data is weaker than the one of the theoretical calculation, which suggests that the increase of the scaling function, due to the decrease of k_{min} with q , is almost balanced by its decrease due to FSI. In a recent paper,¹⁹ a nuclear matter spectral function based on the Brueckner-Bethe-Goldstone theory and modified in order to be used for finite nuclei, has been employed in the calculation of ${}^{56}\text{Fe}$ scaling function, with results exhibiting the same qualitative trend as the one shown in Fig. 2, in particular the nonsaturating behavior of the calculated scaling function at large values of y .

The q behavior of the scaling function for ${}^{56}\text{Fe}$ for fixed values of y , is presented in Fig. 3. It can be seen that, at high values of $|y|$, the experimental data do not scale and that the theoretical asymptotic scaling function is still lower than the experimental data at the highest value of q . The value of the asymptotic experimental scaling function obtained in Ref. 17 is, however, in close agreement with the corresponding theoretical value. In Ref. 20, a realistic nuclear matter calculation of the scaling function including FSI within the linked cluster expansion has been reported. At high values of the momentum transfer, FSI effects have been found to vanish, and the scaling func-

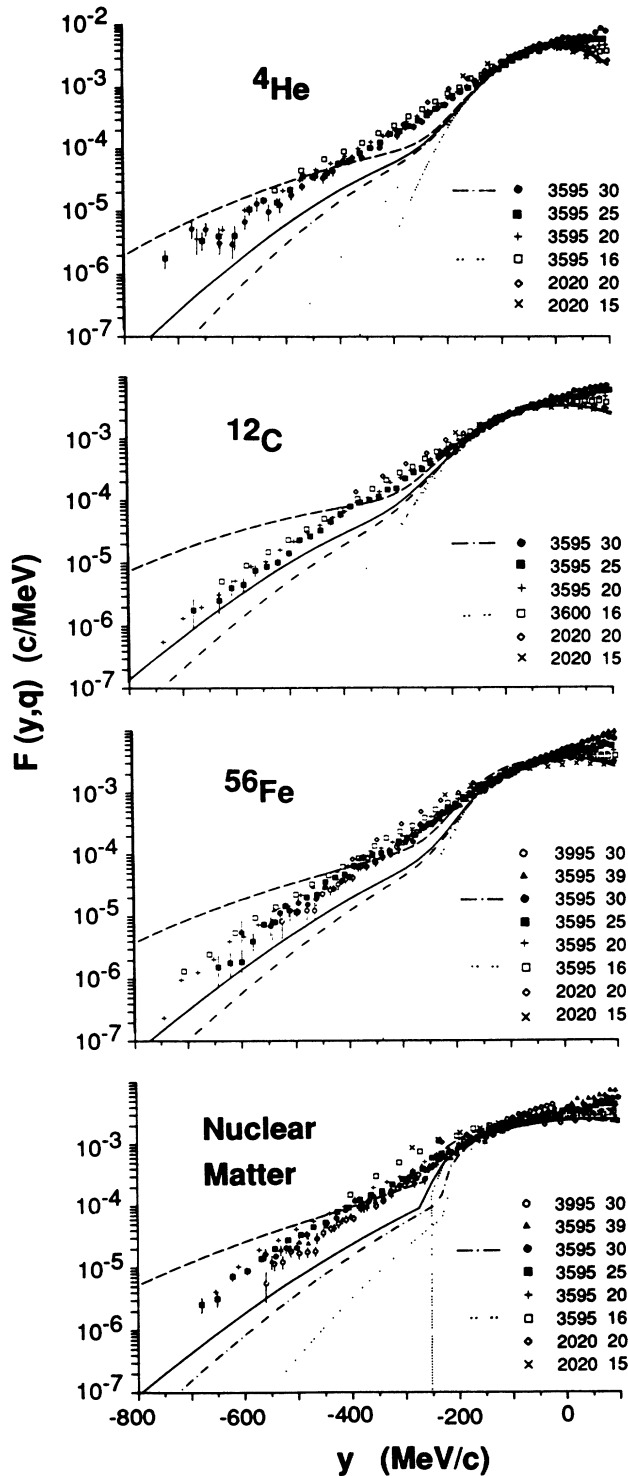


FIG. 2. Comparison between the experimental scaling function [Eq. (15)] obtained in Ref. 17 with theoretical calculations performed with the spectral function defined by Eqs. (1), (2), (5), and (7). The dotted line represents the one-body contribution [first term of Eq. (9)], whereas the double-dotted and dash-dotted lines include also the many-body contribution [second term of Eq. (9)], corresponding to the kinematics shown in the inset. The solid line is the asymptotic scaling function (12) and the dashed line the longitudinal momentum distribution (14). The Hartree-Fock results for finite nuclei are represented by the dotted lines divided by 0.8.

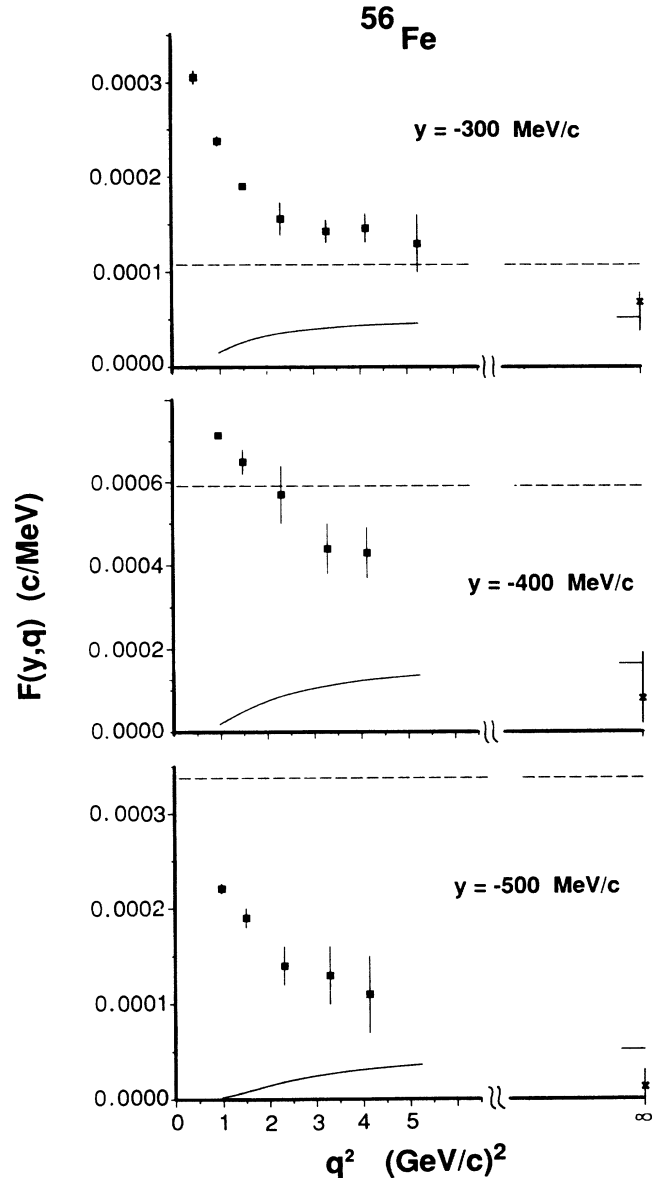


FIG. 3. The experimental scaling function of ${}^{56}\text{Fe}$ (Ref. 17) compared with the longitudinal momentum distribution (14) (dashed line) and the asymptotic scaling function (12) (solid line). The stars with error bars represent the value of the experimental scaling function extrapolated in Ref. 17 to $q \rightarrow \infty$, which is believed to represent the experimental asymptotic scaling function.

tion, which turned out to approach the longitudinal momentum distribution, has been found to be sensibly higher than the experimental points. According to our calculations, the latter result should be ascribed to the absence of binding effects in the approach of Ref. 20; as a matter of fact, it can be seen from Fig. 3, that when the spectral function is used, the asymptotic scaling function is sensibly lower than the experimental data.

Several approximated forms for P_1 have recently been employed in the calculations of inclusive processes at high energy and momentum transfer;^{9,16} in particular two models have been considered: (i) the δ -function model in

which only the mean value of the energy associated with the excited configurations is taken into account, viz., $P_1(k, E) = n_1(k) \delta(E - \bar{E}_1)$, where \bar{E}_1 can readily be found from the energy sum rule (for details see Ref. 9); (ii) the δ -function model with two-nucleon correlations, viz., $P_1(k, E) = n_1(k) \delta(E - E_1(k))$, with $E_1(k)$ being the solution of Eq. (6). In Fig. 4, the asymptotic scaling function (12) predicted by these models is compared with the one obtained by model (7). It can be seen that at high negative values of y the δ -function models yield totally different results with respect to the model in which the energy dependence of the spectral function for $E \neq E_1(k)$ is taken into account.

In conclusion, we would like to point out once again that: (i) The calculation of quasielastic electron scattering at high values of y has to be performed in terms of the spectral function and not in terms of the momentum distribution only; to this end the model developed in Ref. 7 and in this paper represents a valid candidate for complex nuclei [note that the finite widths of the hole states, disregarded in Eqs. (2) and (5), slightly affect the *inclusive* cross section only at $y \approx 0$ without any appreciable change of our results]. (ii) Even when binding effects are taken into account, a sizable discrepancy between PWIA predictions and the experimental points at the highest value of the momentum transfer, remain to be explained; such a discrepancy, which is present even in the exact treatment for deuteron and ^3He ,¹⁶ should not be ascribed to some inadequacies of the used spectral function for complex nuclei, but to the presence of FSI which seem to affect present experimental data even in the region of the

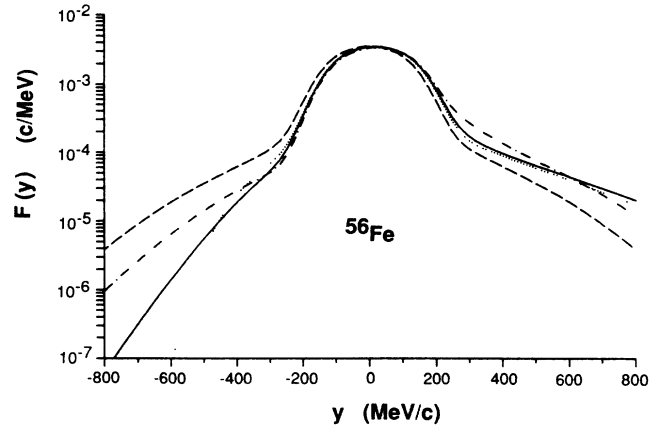


FIG. 4. The asymptotic scaling function of ^{56}Fe [Eq. (12)] calculated with different model spectral functions for P_1 , with P_0 given by Eq. (2). Dotted line: $P_1(k, E) = n_1(k) \delta(E - E_1(k))$; dash-dotted line: $P_1(k, E) = n_1(k) \delta(E - \bar{E}_1)$; solid line: Eq. (7). The dashed line represents the longitudinal momentum distribution (14).

highest momentum transfer. Progress has already been done to develop a realistic treatment of FSI,²⁰ but further efforts are necessary in order to take binding effects (NN correlations) and FSI into account simultaneously.

We would like to thank O. Benhar, D. B. Day, L. Frankfurt, E. Pace, G. Salmè, and M. Strikman for discussions on different aspects of this work.

¹G. B. West, Phys. Rep. **18**, 263 (1975).

²C. Ciofi degli Atti, Lett. Nuovo Cimento **41**, 330 (1983).

³E. Pace and G. Salmè, Phys. Lett. **110B**, 441 (1982).

⁴D. B. Day, J. S. McCarthy, Z. E. Meziani, R. Minehart, R. Sealock, S. T. Thornton, J. Jourdan, I. Sick, B. W. Filippone, R. D. McKeown, R. G. Milner, D. H. Potterveld, and Z. Szalata, Phys. Rev. Lett. **59**, 427 (1987); D. B. Day (private communication).

⁵D. B. Day, J. S. McCarthy, Z. E. Meziani, R. Minehart, R. Sealock, S. T. Thornton, J. Jourdan, I. Sick, B. W. Filippone, R. D. McKeown, R. G. Milner, D. H. Potterveld, and Z. Szalata, Phys. Rev. C **40**, 1011 (1989).

⁶X. D. Ji and J. Engel, Phys. Rev. C **40**, R497 (1989).

⁷C. Ciofi degli Atti, L. Frankfurt, S. Simula, and M. Strikman, in *Perspectives in Nuclear Physics at Intermediate Energies*, edited by S. Boffi, C. Ciofi degli Atti, and M. M. Giannini (World Scientific, Singapore, 1989), p. 312; and (unpublished).

⁸L. L. Frankfurt and M. I. Strikman, Phys. Rep. **76**, 217 (1981); **160**, 236 (1988).

⁹C. Ciofi degli Atti and S. Liuti, Phys. Lett. B **225**, 215 (1989).

¹⁰C. Ciofi degli Atti, E. Pace, and G. Salmè, Phys. Lett. B **141**, 14 (1984).

¹¹O. Benhar, A. Fabrocini, and S. Fantoni, Nucl. Phys. **A505**, 267 (1989); in *Perspectives in Nuclear Physics at Intermediate Energies*, edited by S. Boffi, C. Ciofi degli Atti, and M. M. Giannini (World Scientific, Singapore, 1989), p. 333.

¹²D. S. Koltun, Phys. Rev. C **9**, 484 (1974).

¹³Y. Akaishi, Nucl. Phys. **A416**, 409c (1984); and (private communications); R. Schiavilla, V. R. Pandharipande, and R. B. Wiringa, Nucl. Phys. **A449**, 219 (1986).

¹⁴O. Benhar, C. Ciofi degli Atti, S. Liuti, and G. Salmè, Phys. Lett. B **177**, 135 (1986); C. Ciofi degli Atti, O. Benhar, and G. Salmè, in *The Fourth Amsterdam Miniconference on Nuclear Structure in the 1p Shell, 1986*, edited by L. Lapikas, H. de Vries, and C. de Vries (NIKHEF, Amsterdam, 1986), p. 209.

¹⁵S. Frullani and J. Mougey, Adv. Nucl. Phys. **14**, 1 (1984).

¹⁶C. Ciofi degli Atti, E. Pace, and G. Salmè, Phys. Lett. **127B**, 303 (1983); Phys. Rev. C **36**, 1208 (1987); **39**, 259 (1989).

¹⁷C. Ciofi degli Atti, E. Pace, and G. Salmè, Nucl. Phys. **A497**, 361c (1989); **A508**, 349c (1990); Phys. Rev. C **39**, 259 (1989); and (unpublished).

¹⁸T. de Forest, Jr., Nucl. Phys. **A392**, 232 (1983).

¹⁹X. D. Ji and R. D. McKeown, Phys. Lett. B **236**, 130 (1990).

²⁰M. N. Butler and S. E. Koonin, Phys. Lett. B **205**, 123 (1988).